Hydropedology Symposium: 10 Years Later and 10 Years into the Future

Frequency and Control of Subsurface Preferential Flow: From Pedon to Catchment Scales

Hu Liu Henry Lin*

Dep. of Ecosystem Science and Management Pennsylvania State Univ. University Park, PA 16802 Quantitative assessment of frequency and control of preferential flow (PF) across the landscape has been largely lacking. Previous work evaluated PF occurrence at 10 sites along a hillslope in the Shale Hills Catchment using soil moisture response to 175 precipitation events. We expanded the analysis to include (i) 237 additional events to test the temporal consistency and predictability of PF occurrence and (ii) 25 additional sites to upscale to the entire catchment. The results showed considerable temporal consistence in both frequency and main controls of PF at the hillslope scale, attributed largely to statistical stability of precipitation patterns during the 6.5-yr monitoring and relatively stable subsurface PF paths. Generally, PF tended to occur more often in response to intense rainfalls and favored conditions at dry hilltop or wet valley sites. When upscaling to the catchment, topographic controls became more evident, leading to the identification of a hidden subsurface PF network. Higher frequency of PF occurred at the hilltop (average 46%) and the valley floor (average 41%), while the overall average frequency for swales was 26% and that for planar and convex hillslopes was 18%. Soil-terrain attributes provided a limited estimation ($R^2 = 0.43-0.48$) of PF occurrence, suggesting complexities involved in PF dynamics. This study confirmed that the initiation and persistence of PF were controlled by interactions among landforms, soils, initial moisture conditions, precipitation, and seasons. Further investigations of these key controls can lead to improved understanding and modeling of PF from pedon to catchment scales.

Abbreviations: API, antecedent precipitation index; CPI, current precipitation index; PF, preferential flow.

Preferential flow (PF), the process in which water bypasses a portion of the soil matrix through various mechanisms, can lead to faster and deeper water flow and solute transport than what would be expected by the classical flow theory (Hendrickx and Flury, 2001; Šimůnek and van Genuchten, 2007). Subsurface PF has been recognized as a key process in catchment hydrology and is believed to be ubiquitous (Uhlenbrook and Wenninger, 2006; Doerr et al., 2007; Lin, 2010). Locally, PF impacts infiltration, soil water storage, runoff generation, filter and buffer functions, and slope stability (Uchida et al., 2001; Lago et al., 2010; Chappell, 2010; Alaoui et al., 2011), while regionally it affects the hydrologic cycle and biogeochemical cycling (Jaynes et al., 2001; McClain et al., 2003; Jarvis, 2007; Clothier et al., 2008; Posadas et al. 2009). Characterization of PF at multiple spatial and temporal scales is thus fundamental to the understanding of complex subsurface hydrology and is essential to reliable modeling and prediction of hillslope and catchment processes (Lin and Zhou, 2008; Allaire et al.,

Soil Sci. Soc. Am. J. 79:362–377 doi:10.2136/sssaj2014.08.0330

Received 21 Aug. 2014.

Accepted 8 Jan. 2015.

*Corresponding author (henrylin@psu.edu).

© Soil Science Society of America, 5585 Guilford Rd., Madison WI 53711 USA

All rights reserved. No part of this periodical may be reproduced or transmitted in any form or by any means, electronic or mechanical, including photocopying, recording, or any information storage and retrieval system, without permission in writing from the publisher. Permission for printing and for reprinting the material contained herein has been obtained by the publisher.

2009). Despite the importance of PF, its occurrence, frequency, controls, and locations in various landscapes remain unclear (Graham and Lin, 2011).

Soil moisture responds to rainfall events in many different ways due to the heterogeneity of soils, landforms, vegetation, and precipitation (Alaoui et al., 2011). When scaling up from the pedon to the landscape scale, factors such as topography, landform unit, vegetation, and soil properties influence the initiation and continuation of PF because of spatially variable site characteristics (Kulasekera and Parkin, 2011), temporally variable moisture conditions (Kienzler and Naef, 2008), and complex interactions between them (Zehe and Sivapalan, 2009).

As a result, PF is difficult to measure and quantify, and its temporal-spatial pattern has been hard to predict (Šimůnek et al., 2003; Scherrer et al., 2007). Traditionally, field-scale PF occurrence has been investigated by combining tracer studies with flow experiments or lysimeter or tile drainage (Weiler and Flühler, 2004; Allaire et al., 2009; Anderson et al., 2009). Recently, ground penetrating radar, electromagnetic induction, and other geophysical techniques have been used to observe and quantify PF with minimal soil disturbance (Garré et al., 2010; Oberdörster et al., 2010; Sammartino et al., 2012; Zhang et al., 2014; Guo et al., 2014). While these methods can effectively demonstrate the spatial occurrence of PF, they are less effective in determining the temporal pattern of PF (Graham and Lin, 2011). Increased deployment of extensive soil moisture sensor networks has offered an opportunity to address both the temporal dynamics and spatial pattern of PF (Kienzler and Naef, 2008; Blume et al., 2009; Graham and Lin, 2011).

Through the use of soil moisture sensor networks, our previous work has identified two types of PF that affect different parts of the forested Shale Hills Catchment: vertical flow via macropores, cracks, hydrophobicity, or other PF paths under dry conditions, and lateral subsurface flow during large precipitation events in wet soils or during snowmelt, especially in the valley and swales (Lin and Zhou, 2008). Graham and Lin (2011) extended this analysis to include 3 yr (2007–2009) of soil moisture response to various precipitation events and found that PF occurred during 17 to 54% of 175 events at each of 10 monitored sites along a hillslope in this catchment. They also reported that, while the frequency of PF appeared insensitive to topographic position, the controls on PF initiation varied with landscape position. Zhao et al. (2012) compared the occurrence frequency and the control of PF in two contrasting landscapes (forested vs. cropped lands) and found that the spatial complexity and temporal dynamics of PF were controlled by the interactions among terrain, soils, and vegetation and that such interactions changed with seasonal wetness, precipitation characteristics, landscape locations, and soil depth.

This study expands on the work of Graham and Lin (2011) with the additional analysis of 237 precipitation events occurring from 2010 to 2013 (yielding a total of 412 precipitation events during 6.5 yr) and 25 more sites covering the entire catchment. This study was motivated by a desire to estimate the spatial-temporal likelihood of PF occurrence in the Shale Hills Catchment.

Of particular interest is the frequency and control of PF occurrence at various temporal and spatial scales. Two hypotheses investigated were:

- There is a temporal consistency in long-term PF occurrence frequency at a specific site, and the controlling factors and spatial pattern of PF occurrence have some degree of stability and thus predictability. If this is true, then statistical results would be similar between different time periods for the same sites.
- 2. Spatial dependence in PF occurrence and its frequency may not necessarily be significant at the hillslope scale in complex terrains but becomes more evident at the catchment scale that encompasses various landform units. If this is true, then some spatial patterns of PF occurrence should become clearer when upscaling the observations of PF from the hillslope scale to the catchment scale.

Through this expanded study, we discern the dominant controls of PF occurrence, both temporally and spatially, and further reveal how precipitation features, initial soil moisture conditions, terrain attributes, and soil properties affect PF occurrence from pedon to catchment scales.

MATERIALS AND METHODS Site Description

The Shale Hills Catchment is a US National Critical Zone Observatory located in central Pennsylvania. This 7.9-ha forested catchment is characterized by steep slopes (up to 48%) and narrow ridges, with elevation ranging from 256 to 310 m. There are five dominant landform units (valley, swale, planar hillslope, convex hillslope, and ridgetop) and five typical soil series (the Weikert, Berks, Rushtown, Ernest, and Blairton series) in the catchment (Lin, 2006). Swales (concave hillslopes) are dispersed on both sides of a first-order stream in the catchment, with five on the south-facing slope and two on the north-facing slope. The soils were derived from Silurian-age shale, with texture generally being silt loam and silty clay loam, with some clay loam and sandy clay loam. The Weikert soil series is a shallow (<0.5-m depth to bedrock), well-drained soil on steep planar hillslopes or ridgetops; the Berks series is a moderately deep (0.5-1.0-m depth to bedrock), well-drained soil on the toeslope and sideslope of concave hillslopes; the Rushtown series is a deep (>1-m depth to bedrock), well-drained soil at the center of concave hillslopes; the Ernest series is a very deep (>3-m depth to bedrock), poorly to moderately well-drained soil on the valley floor around the first-order stream; and the Blairton series is also a very deep (>3-m depth to bedrock), moderately well-drained soil found at the east end of the catchment valley floor (Fig. 1).

The climate at the Shale Hills is typical of a humid temperate region, with long-term (>100 yr) mean monthly temperatures reaching a minimum of -3° C in January and a maximum of 22° C in July. Annual precipitation is around 980 mm (National Weather Service, State College, PA), which is almost evenly distributed during the year, with a maximum in summer. Precipitation during the

summer months usually occurs as convective storms of higher intensity and shorter duration. Several species of maple (*Acer* spp.), oak (*Quercus* spp.), and hickory (*Carya* spp.) are typical deciduous trees found on the sloping areas and on ridges, while the valley floor is dominated by eastern hemlock (*Tsuga canadensis* Carriére) (Lin, 2006; Takagi and Lin, 2011).

Field Measurements

Soil moisture data have been collected in the Shale Hills using an automatic sensor network. This includes 10 sites that have been operating since September 2006 and 25 additional sites since May 2011. Capacitance-type soil moisture probes (ECH₂O-5, ECH₂O-10, and later 5TE and 5TM, Decagon Devices Inc.) were installed in various soil horizons or at their interfaces from the soil surface down to the soil-bedrock interface (or as deep as could be excavated safely). The depth and number of probes installed were based on soil thickness and horizonation, which varied among the soil series (Table 1). The shallowest probe at each site ranged from 5 to 15 cm, while the deepest ranged from 37 to 162 cm. All the probes were installed at the upslope side of excavated soil pits, which were then carefully backfilled with the original soil layer by layer to maintain their original setting and minimize the effects of disturbance associated with the installation. All cables were carefully buried below the depth of the installed probes and then laid horizontally away from the probe locations. The selection of the monitoring sites was based on the combined considerations of soil type, landform unit, and terrain attributes so that adequate representation and coverage were achieved.

study, 17 were located on the south-facing hillslopes, 13 on the north-facing hillslopes, and
five on the valley floor (Table 1; Fig. 1). We used one full year of
continuous 10-min time series data from May 2011 through June
2012 for the catchment-scale analysis, except four sites (Sites 15,
61, 49, and A4) that had only 4 to 8 mo of data due to equipment
malfunctions. An additional one full year of data from July 2012
to July 2013 was used for testing predictions. Among the 10 sites
installed earlier for the hillslope-scale study, three, four, and three
sites were in the upper (U), middle (M), and lower (L) portions
of a concave hillslope, respectively. A more detailed description

Among the 35 sites for the catchment-wide

Precipitation has been measured automatically at a 10-min time interval using six rain gauges distributed in the catchment. One main gauge located at the north ridge weather station is a Pluvio load cell rain gauge (OTT Hydrometry; resolution 0.01

of these 10 sites can be found in Graham and Lin (2011).

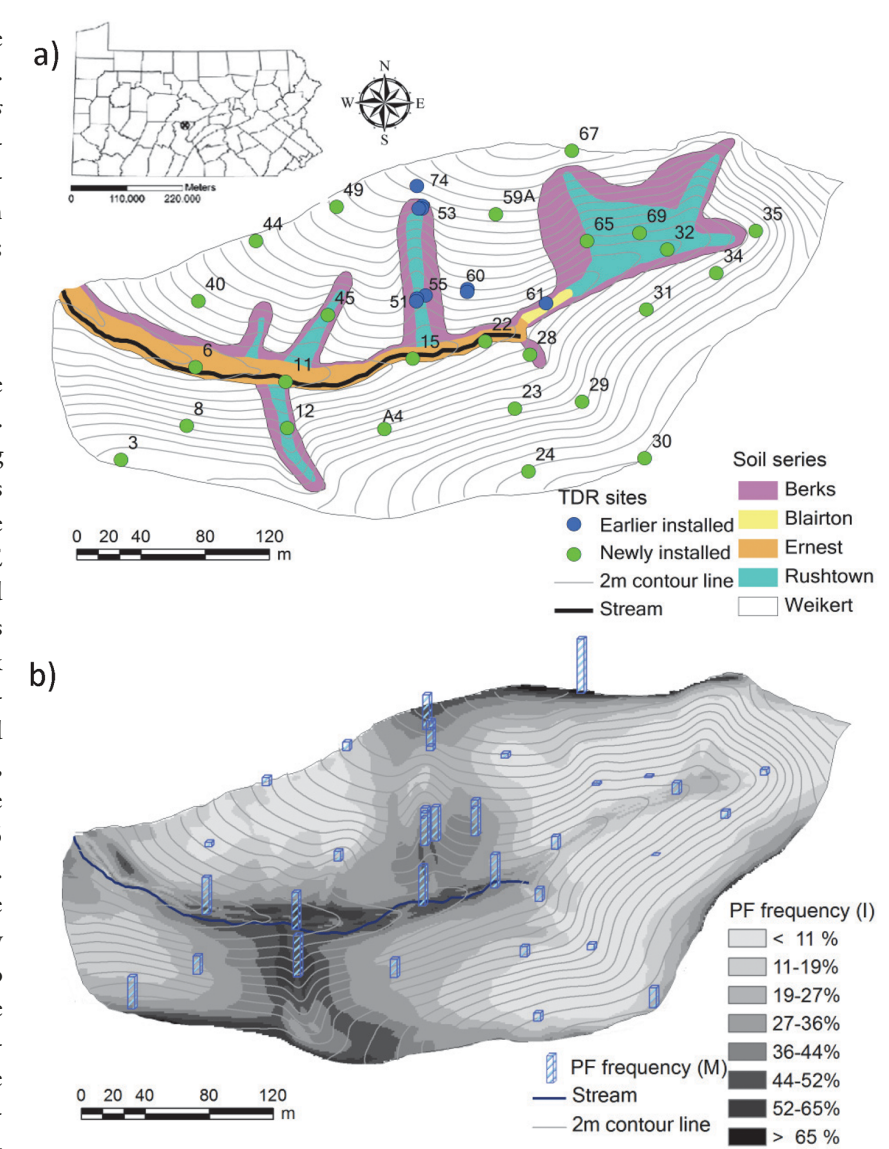


Fig. 1. (a) Location of the Shale Hills Catchment, its soil map, and soil moisture monitoring sites (note that there are multiple sites close to each other at Sites 51, 53, 55, and 60 that are hard to see on the map), and (b) measured (M) and interpolated (I) preferential flow (PF) occurrence frequency based on the data from the period May 2011 to June 2012 for all 35 sites, with all the available data in each soil profile used in estimation (with the bar height representing the size of PF frequency, which ranged from <1% at Site 31 to 70.1% at Site 67). The interpolation map was generated using regression kriging.

mm), while the other five are TE525-WS tipping bucket rain gauges (Texas Electronics; resolution 0.025 mm). Slight differences existed in the precipitation recorded by the various rain gauges, which was partially attributed to canopy influences and occasional clogging by fallen leaves. The rainfall amounts were averaged to provide the catchment-wide rainfall data for the analysis in this study, as justified by Graham and Lin (2011).

Preferential Flow Analysis

The precipitation and soil moisture data at the 10-min time interval were used in the PF analysis reported here. Both the precipitation delineation and the identification of PF occurrence were performed according to the method established by Graham and Lin (2011). Storm events were determined using the precipi-

Table 1. Characteristics of soil moisture monitoring sites and sensor installation depths and horizons in the Shale Hills Catchment. The layout of the sites is shown in Fig. 1. The first 11 sites have data from 2007 to 2013, and the remaining 24 sites have data from 2011 to 2013. Soil horizons in bold in the last column are those that were selected to estimate preferential flow frequency based on three typical soil depths or horizons.

Site no.	Landform unit	Elevation m	Hillslope aspect (facing)	Slope %	Curvature × 10 ⁻³	Soil series	Soil depth	Log of upslope area m ²	Topographic wetness index	Total probes installed	Depths of probes/soil horizon (or horizon interface if two horizons are indicated)
74 (U1)†	convex	295.0	south	22.3	× 10 ³	Weikert	0.20	1.35	4.52	5	5/Oe–A, 8/A, 10/A–CR, 17/CR, 37/R
60 (U2a)	convex	279.9	south	27.5	7.1	Weikert	0.40	1.82	5.41	5	5/Oe–A , 8/A, 21/Bw , 31/Bw–CR , 39/CR–R
60 (U2b)	convex	279.9	south	27.1	0.6	Weikert	0.40	1.82	5.41	5	5/Oe–A , 8/A, 15/Bw , 28/Bw–CR , 38/CR–R
5 (M1)	swale	285.9	south	26.4	-24.7	Berks	>1.50	1.50	4.62	5	14/Bw1, 41/Bw2, 86/Bw3 90/Bw3–CR, 111/C
3 (M2a)	planar	291.1	south	34.0	-21.1	Rushtown	1.10	1.73	5.00	5	5/Oe –A, 10/A , 40/Bw2 , 88/BC–C, 103/C
3 (M2b)	planar	291.1	south	34.3	-27.6	Rushtown	1.50	1.73	5.00	5	5/Oe–A , 10/A , 40/Bw2 , 97/BC–C, 112/C
3 (M2c)	planar	291.1	south	33.5	-26.5	Rushtown	1.50	1.73	5.00	5	10/A , 22/Bw1 , 44/Bw2 , 73/Bw3, 123/C
1 (L1a)	swale	274.9	south	14.3	-46.5	Rushtown	>3.0	2.87	8.82	5	8/A , 18/Bw , 39/Bw3 115/C1–C2, 156/C ₂
1 (L1b)	swale	274.9	south	13.8	-38.1	Rushtown	> 3.0	2.87	8.82	10	5/O , 8/A–Bw1, 12/Bw1, 15/Bw1 , 22/Bw2, 40/Bw3 68/BC, 92/BC–C1, 122/C1 162/C2
1 (L2)	valley	273.8	_	10.4	-54.2	Blairton	>2.5	3.14	9.76	7	13/A, 20/BA, 35/Bt1 , 66/Bt2, 86/Bt2, 95/CB1, 129/CB2
5	valley	268.6	-	3.2	-33.7	Ernest	>3.0	4.27	12.7	7	13/A, 20/AE–Bw, 41/Bt, 52/Bt–C1, 72/C2, 85/C2–C3, 109/C4
	hilltop	283.0	north	9.3	13.6	Weikert	0.33	0.77	4.00	5	5/A , 10/B, 15/C , 20/C, 30/R
	valley	262.3	-	13.2	-1.0	Ernest	1.40	2.62	7.91	5	10/A , 20/B , 30/C , 40/C, 60/R
	convex	274.7	north	41.6	5.3	Weikert	0.36	1.60	4.45	5	10/A, 20/B, 30/C , 40/C, 50/R
1	valley	264.9	-	18.4	-14.4	Ernest	1.52	2.75	7.89	3	5/A , 11/A, 15/AE–Bw , 24/Bw, 30/B t, 36/Bt–C1, 51/C1 , 66/C2
2	swale	272.0	north	24.6	-82.0	Rushtown	2.12	2.99	8.21	5	5/O , 10/A, 15/A , 27/Bw, 48/Bt–C1, 50/Bt–C1 64/C1, 81/C2
2A	valley	271.0	-	13.2	-13.4	Ernest	1.52	2.23	6.93	3	5/A, 15/B, 50/C
3	convex	284.6	north	39.7	3.5	Weikert	0.40	2.23	4.68	3	5/A, 15/B, 25/C
4	convex	298.4	north	18.8	15.2	Weikert	0.30	1.22	4.42	3	5/A, 15/B, 25/C
8	swale	274.9	north	21.1	-51.1	Berks	0.90	3.18	8.77	3	5/A, 15/B, 50/C
9	planar	287.3	north	23.7	-22.1	Weikert	0.65	2.62	7.39	3	5/A, 15/B, 25/C
)	hilltop	299.7	north	10.0	9.4	Weikert Weikert	0.30	0.90	4.26	3	5/A, 15/B, 30/C 5/A, 15/B, 50/C
1 <u>2</u>	convex swale	286.3 279.2	north south	37.3 6.7	-2.4 -48.9	Rushtown	0.37 1.52	1.75 3.58	4.90 10.66	3	5/A, 15/B, 50/C
<u>2</u> 4	convex	288.1	north	37.4	-46.9 1.2	Weikert	0.50	1.58	4.52	3	5/A, 15/B, 50/C
5	planar	287.4	north	25.5	-58.7	Weikert	0.66	2.57	7.16	3	5/A, 15/B, 30/C
)	convex	270.4	south	20.4	4.0	Weikert	0.22	1.56	5.08	3	5/A, 15/B, 30/C
4	planar	279.4	south	16.6	-0.6	Weikert	0.38	1.32	4.71	3	5/A, 15/B, 30/C
5	swale	271.5	south	23.7	-81.2	Rushtown	1.67	2.70	7.53	3	5/A, 15/B, 30/C
9	convex	288.6	south	14.4	14.2	Weikert	0.35	1.12	4.39	3	5/A, 15/B, 30/C
9A	convex	293.6	south	27.6	-3.6	Weikert	0.20	1.54	4.74	3	5/A, 15/B, 30/C
5	swale	281.6	north	34.5	-35.5	Rushtown	3.00	2.21	6.03	3	5/A, 15/B, 50/C
7	hilltop	301.4	south	7.5	31.1	Weikert	0.10	0.47	3.60	3	5/A, 15/B, 25/C
9	swale	282.1	south	36.0	-4.9	Rushtown	1.09	1.77	4.99	3	5/A, 15/B, 50/C
4	convex	280.4	north	38.5	6.7	Weikert	0.38	1.66	4.67	3	5/A, 20/B, 35/C

+ Soil profile label in parentheses.

tation: individual events were delineated based on >1 mm of total precipitation falling after >24 h of no rainfall. Once a precipitation event began, it was considered to continue until the total precipitation in any given 24-h period was <1 mm. The 1-mm precipitation threshold and the minimum of 24 h between event periods were determined by testing and precipitation pattern analysis described by Graham and Lin (2011). Events of <1 mm were not delineated in this study, and the delineated events with an average air temperature <1 $^{\circ}$ C or with apparent clogging of rain gauges were removed from the data set. A total of 175 events were included for the period from 2007 to 2009 and an additional 148 events were included for the period of 2010 to 2012 (Fig. 2). For testing the predictability of PF occurrence, 89 additional precipitation events from 2012 to 2013 were used.

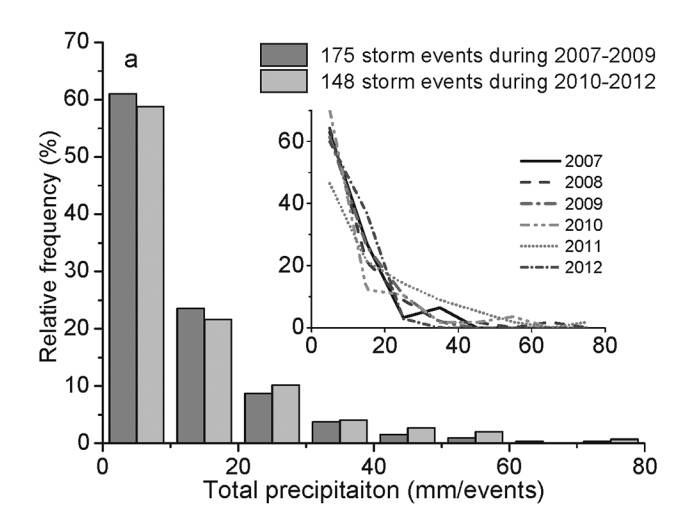
Once the precipitation events were determined, the soil moisture time series at each site was examined. Soil moisture time series at each site and each depth were used to determine the sequence of soil moisture probe response to each precipitation event within each site. If volumetric soil moisture content increased above the threshold value of 1% (v/v) (for detailed justification of this value, see Lin and Zhou, 2008), the time of the initial rise was recorded. Once each probe response time to a precipitation event was determined, the soil moisture response sequence throughout each soil profile was then classified into three general categories of flow regime: sequential, preferential, and nondetectable based on the following criteria (for further justification, see Graham and Lin, 2011):

- Sequential flow includes events where probes at various soil depths responded in a sequential order from the surface down to the deepest probe.
- Preferential flow includes events where at least one deeper probe responded to a precipitation input earlier than a shallower probe or where shallow and deep probes responded sequentially but a probe in between them did not respond.
- Nondetectable flow includes events where the precipitation amount either was insufficient to trigger a soil moisture response even at the uppermost probe or was removed by evapotranspiration before percolation could reach any of the installed probes.

The frequency of PF occurrence reported in this study should be considered as a lower bound (i.e., probably underestimated) (Graham and Lin, 2011). This is because of the following two possible scenarios of PF that were not discerned in our analysis: (i) a flow that bypassed all of the soil moisture sensors, and thus a nondetectable flow does not necessarily preclude the possibility of PF; and (ii) a rapid, sequential soil moisture response to precipitation may also suggest a PF due to wave propagation or high soil permeability.

Statistical Analysis

The 10 sites investigated by Graham and Lin (2011) were used to conduct temporal consistency analysis for the time pe-



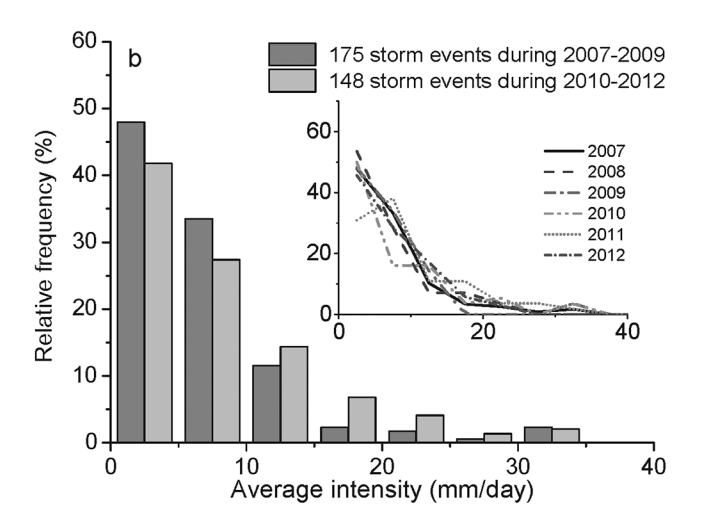


Fig. 2. Frequency distribution of (a) total precipitation per event and (b) average precipitation intensity for the periods of 2007 to 2009 (dark gray) and 2010 to 2012 (light gray). The insets are the distribution curves for each individual year's precipitation events (four events with an average intensity of >100 mm d⁻¹ are not shown but were included in the analysis).

riods of 2007 to 2009 (3 yr) vs. 2007 to 2012 (5.5 yr) as well as spatial dependency analysis at the hillslope scale. Matched-pair ttests were performed to examine the differences in the frequency of PF occurrence. All the precipitation indices and initial soil moisture indices used by Graham and Lin (2011) were used in this study. A total of 33 precipitation indices, grouped roughly into three categories (antecedent precipitation, event characteristics, and timing of precipitation), were derived for the period of January 2007 to June 2012, along with 8 to 14 indices of initial soil moisture conditions (depending on the number of soil depths involved at each site) (Table 2). Antecedent and current precipitation indices (API and CPI, respectively) were used to describe antecedent precipitation, with API estimated as the total precipitation in a given number of days before a storm event (e.g., 1-14-d APIs, denoted as API 1-API 14, respectively), and CPI was calculated as CPI(t) = α CPI(t – 1) + P(t), where α is a coefficient, t is the time step, and P(t) is the precipitation at time t, with values of α set at 0.9 (CPI9), 0.99 (CPI99), and

0.999 (CPI999). Indices for event characteristics included total event precipitation, event duration, maximum and average intensity, average intensity from the start to the time of maximum intensity, and variance, skew, and kurtosis of the precipitation distribution for each event. Precipitation timing indices included the day of the year of event initiation, mean air temperature for the event duration, and the time between events. Indices describing the initial soil moisture included average soil moisture at different depths (3–10 depths at each site, depending on soil type and horizonation; see Table 1), profile average, and depthweighted average of soil moisture content. These soil moisture indices were estimated based on the soil moisture readings during the 3-h time before the start of a storm event.

All the above indices were sorted according to the determined flow categories, and then the means were statistically compared using a t-test. Indices for events that produced PF vs. sequential flow (SF) were placed in two separate bins, and a t-test was performed to indicate whether there were any significant differences (p < 0.05) between the set of events that resulted

in PF and the events that resulted in SF. Precipitation events where a large number of sites responded with either PF or SF were also identified and the characteristics of the two data sets were statistically compared to determine how the indices affect the widespread occurrence of PF across the hillslope or catchment scales (Table 2). The degree of agreement of the indices controlling PF occurrence was tested by comparing the subsets of time series with the controls found for the entire monitoring data set. A value of 100% indicates that the indices that were determined to control PF for the selected subset coincided with those determined from the entire data set. No agreement would suggest that all the significant controls determined from the entire time series were found insignificant for the chosen subset and vice versa. A null hypothesis was set that none of the indices was a significant control (that is, PF is completely random and not dependent on any of the proposed indices) (Graham and Lin, 2011).

All 35 sites were used in the spatial dependence analysis at the catchment scale. The frequency of PF occurrence at each of these sites was determined for the period from May 2011 to June

Table 2. Selected indices of precipitation (ppt) and initial volumetric soil moisture content (θ) for events that resulted in preferential flow (PF) at individual and multiple sites at the hillslope scale. Individual sites are organized from hilltop to hill bottom, with the ridgetop and hillslope sites (U1, U2a, and U2b) to the left of the midslope sites (M1, M2a, M2b, and M2c), which are to the left of the lower swale and valley sites (L1a, L1b, and L2). Indices with significant p values (95% confidence interval) from t-tests for the 175 precipitation events of 2007 to 2009 and the 323 precipitation events of 2007 to 2012 are marked. A dash indicates that the indices were not tested. Empty cells indicate that the indices were not statistically significant.

	Significant in controlling PF at individual sites											Significant in controlling PF at \geq 3–6 sites				
Index†	U1	U2a	U2b	M1	M2a	M2b	M2c	L1a	L1b	L2	≥3 sites	≥4 sites	≥5 sites	≥6 sites		
Total ppt					‡	§		¶	§	‡	§		§	§		
Ppt duration		\P			‡	‡			§				§	§		
Avg. ppt intensity					‡		¶	\P								
Max. ppt Intensity						§	§									
Time to max. ppt intensity				\P	§	§			‡				§	#		
Ppt amount to max. intensity					‡			\P	‡	#				‡		
Avg. intensity to max. intensity					‡			\P	‡	‡				‡		
Skew	#	‡			‡	‡	‡	§		#						
Kurtosis		\P			\P	‡	‡	§		\P						
Max. event CPI999					§	‡		\P	§	#			§	§		
Time to max. event CPI9				‡	§	§			§		§	§	#	#		
Time to max. event CPI99				‡	§	§		\P	§		§	§	§	§		
Time to max. event CPI999		\P			§	§		\P	§				§	§		
API1	#			‡			‡			§	‡	#	#	#		
CPI99	§			‡			‡			§	‡	#	#	#		
Air temperature	#	‡	\P	§	‡	‡	‡			#						
Day of year	\P	‡	#	§			§		#		#	#	‡	‡		
Initial average θ	#	‡	#			§		‡	‡		‡	#	#	#		
Initial depth-weighted avg. θ	#	‡	#			‡		‡	‡		‡	#	#	#		
Horizon 1, initial θ	#	‡	#	§		§	§	‡	‡	#	_	_	_	-		
Horizon 2, initial θ	#	\P	#		§	‡		‡	§	§	_	_	_	-		
Horizon 3, initial θ	\P	\P	#	§	‡	#	\P	\P	§	‡	-	_	_	_		
Horizon 4, initial θ	\P	\P	#		‡	‡	¶	‡	§	§	_	_	_	-		
Horizon 5. initial θ		¶	#	§	#	#	¶		#	§	_	_	_	_		

[†] Event CPI999, internal event current precipitation index (Event CPI) with recession coefficient of 0.999; CPI9 to 999, current precipitation index (CPI) with recession coefficient of 0.9 (CPI99), 0.99 (CPI99), and 0.999 (CPI999), respectively; API 1, antecedent precipitation index (API) for 1 d; Horizons 1 to 5 are numbered sequentially from the soil surface downward to deeper soil where a probe was installed.

[‡] The indices were significant for both periods.

[§] The indices were not significant for the period of 2007–2009 but were significant for the period of 2007–2012.

[¶] The indices were significant for the period of 2007–2009 but not significant for the period of 2007–2012.

2012 (69 events in total) and then tested with the data set for the period from July 2012 to July 2013 (87 events in total). These 35 sites were examined for differences in PF occurrence frequency among different landform units, soil series, and hillslope aspects (north- vs. south-facing) via Duncan's multiple range tests. All the primary topographic attributes (elevation, slope, curvature, and upslope contributing area) and one composite topographic attribute (topographic wetness index) were derived for the whole catchment using a digital elevation model used by Takagi and Lin (2012). We extracted these terrain attributes at all monitoring sites by using the coordinates obtained from the total station survey. Soil properties (e.g., soil depth, profile-averaged sand, silt, clay, organic C, and rock fragment contents) were directly adopted from Takagi and Lin (2012). Spearman correlation analysis was conducted to examine the possible association between PF frequency and the extracted terrain or soil attributes. To evaluate the potential effects of sensor numbers on the measured PF occurrence across the catchment, we also calculated the PF frequencies at the 35 sites with the soil moisture data recorded at three selected horizons representing similar depths (Table 1). A regression kriging (Hengl et al., 2007) with selected terrain attributes and soil properties was then used to generate interpolated maps of PF occurrence frequency across the entire catchment (Fig. 1b). This interpolation method was selected based on our previous investigations (Zhu and Lin, 2010).

To investigate the predictability of PF occurrence in this catchment, we used a stepwise regression algorithm to select soil-terrain attributes based on the past several years' data (i.e., 2007–2012 for the hillslope scale and 2011–2012 for the catchment scale) and then compared the predictions with the latest field data from July 2012 to July 2013. The regression model selection was based on the Akaike information criterion (AIC) coded in R software (R Development Core Team, 2005), where competing models were ranked for a given data set (i.e., 10 sites for the hillslope scale or 35 sites for the catchment scale), and the one with the lowest AIC value was considered as the most appropriate (Venables and Ripley, 2002). Values of t from the multiple

regression were then used to assess the relative importance of the selected variables in predicting the PF occurrence frequency (Kemper and Koch, 1966).

RESULTS Temporal Analysis at the Hillslope Scale

Precipitation at the Shale Hills was dominated by small events (total precipitation <20 mm and average intensity $<10 \text{ mm d}^{-1}$), as shown in Fig. 2. Year-by-year variance existed in the events distribution, but only minor differences were detected between the 2007 to 2009 and 2010 to 2012 periods, i.e., the period of 2010 to 2012 had slightly lower percentages of small and less intense events than the period of 2007 to 2009 (Fig. 2). Of the 323 total delineated precipitation events from 2007 to 2012, 16 to 47% were identified as generating PF at each of the 10 monitoring sites at this hillslope scale (Table 3). This is fairly consistent with the results for the 175 events from the 2007 to 2009 period as reported by Graham and Lin (2011). More frequent PF occurred during either the dry season (June-November) or wet season (December-May) at different sites (Fig. 3), which was associated with hydrophobicity in the dry forest floor or a more connected subsurface network under wet conditions (Lin and Zhou, 2008). While PF occurrence in at least one site in this hillslope was frequent (average 91% during 5.5 yr), widespread PF occurrence across the whole hillslope was much less common (e.g., only 2% of delineated events triggered PF at ≥ 8 sites) (Table 3). For individual sites, some indices appeared to control the PF occurrence across the hillslope (e.g., precipitation skewness, initial soil moisture in upper horizons, and air temperature, which were significant at ≥ 6 sites). Some indices, however, were controlling factors at only few sites (e.g., antecedent precipitation indices, API 2 to API 7, and average or maximum precipitation intensity, which were significant at one or two sites) (Table 2). Only a few indices were consistent controls of PF occurrence (at $\geq 3-6$ sites), such as total precipitation, API 1, CPI99, timing to the maximum event CPI, day of year, and initial soil moisture in upper layers.

Table 3. Percentage of precipitation events leading to each of the three flow regimes (preferential flow, sequential flow, and non-detectable response) at each of 10 monitoring sites installed before 2011 (upper panel) and for different numbers of sites in the same hillslope (lower panel). Sites are organized from hilltop to hill bottom, with the ridgetop and hillslope sites (U1, U2a, and U2b) to the left of the midslope sites (M1, M2a, M2b, and M2c), which are to the left of the lower swale and valley sites (L1a, L1b, and L2).

		Percentage of events resulting in each flow scenario												
Flow type	U1	U2a	U2b	M1	M2a	M2b	M2c	L1a	L1b	L2				
					o	/o ———								
Preferential flow	45 (53)†	31 (30)	47 (42)	27 (18)	45 (52)	29 (36)	16 (21)	31 (23)	47 (54)	24 (34)				
Sequential flow	16 (22)	48 (61)	29 (41)	25 (33)	20 (20)	34 (35)	46 (53)	38 (46)	20 (18)	44 (43)				
Nondetectable	20 (17)	13 (9)	17 (17)	46 (50)	30 (27)	30 (29)	32 (26)	29 (27)	31 (25)	16 (23)				
	≥1 site	≥2 sites	≥3 sites	≥4 sites	≥5 sites	≥6 sites	≥7 sites	≥8 sites						
Preferential flow	91 (90)	76 (82)	63 (69)	49 (50)	33 (38)	20 (22)	8 (10)	2 (4)						
Sequential flow	94 (98)	78 (83)	57 (67)	38 (47)	27 (37)	15 (21)	8 (13)	2 (2)						
Nondetectable	64 (68)	52 (53)	41 (38)	33 (29)	27 (22)	21 (15)	14 (11)	8 (8)						

[†] The first number is the percentage out of the total of 323 precipitation events in the period from January 2007 to June 2012 and the second number (in parentheses) is the percentage of the 175 events that occurred in the period from January 2007 to December 2009 (as reported by Graham and Lin, 2011).

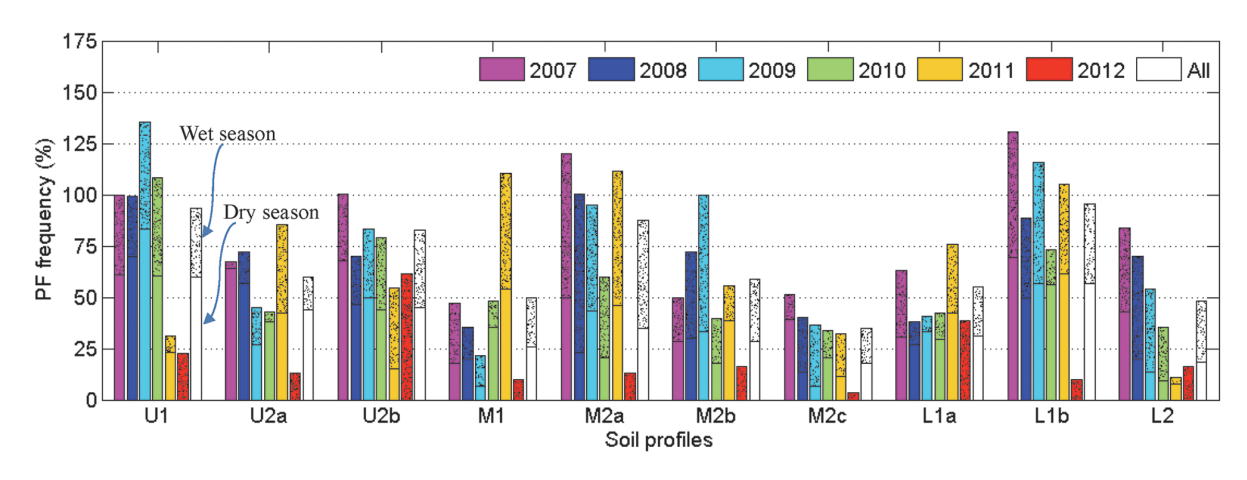


Fig. 3. Frequency of preferential flow (PF) occurrence at each of the 10 monitoring sites at the hillslope scale, expressed as the percentage of total precipitation events that occurred in each of wet or dry season in each of the monitored years from 2007 to 2012. The last bar indicates the overall average during the 5.5 yr, with a total of 323 precipitation events. Each bar is separated into two parts: the upper part (with dots) refers to PF occurrence during the wet season (December–May), while the lower part refers to PF occurrence in the dry season (June–November). Sites are organized from hilltop to hill bottom, with the ridgetop and hillslope sites (U1, U2a, and U2b) to the left of the midslope sites (M1, M2a, M2b, and M2c), which are to the left of the lower swale and valley sites (L1a, L1b, and L2). Note that the entire bar height represents the PF frequency in wet plus dry seasons so the total could be >100%. Among the total 323 precipitation events, 171 occurred during a wet season and 152 occurred during a dry season (data not yet available for the dry season of 2012).

Precipitation and Initial Soil Moisture Control on Preferential Flow Occurrence

While controlling factors of PF occurrence were a mixture across the monitored hillslope, most indices of precipitation characteristics (especially skewness) and timing (especially air temperature) were significant in controlling the occurrence of PF at many individual sites (Table 2). The precipitation characteristics indices were more evident at the middle and lower hillslope sites, while the precipitation timing indices were more common at the upper hillslope sites (Table 2). Among the antecedent precipitation indices, only API 1 and CPI99 were significant for some sites. Most precipitation characteristic indices were also significant in generating widespread PF (at ≥ 6 sites), such as total precipitation, event duration, time to maximum intensity, maximum event CPI999, and time to maximum event CPI9 to CPI999 (Table 2).

Besides precipitation, initial soil moisture also exerted a substantial influence on PF occurrence at both individual sites and across multiple sites. The sites at the upper slope positions (U1, U2a, and U2b) were especially sensitive to initial soil moisture conditions, as well as some sites at the middle- or lower-slope positions (M2b, L1a, and L1b) (Table 2). Similarly, air temperature and the day of the year, which correlated well with initial soil moisture conditions (Graham and Lin, 2011), also appeared to be important controls on PF occurrence at many individual sites. For widespread PF, the dominant control of the overall averaged initial soil moisture was evident (Table 2). Although air temperature was significant in controlling PF at more than six individual sites, it was not significant in generating widespread PF. However, the day of the year appeared to be a significant control for widespread PF (Table 2).

Temporal Variance and Consistence

The frequency of PF occurrence at each site varied from year to year (Fig. 3); however, when looking at a continuous fre-

quency distribution, it was consistent for much of the 5.5-yr monitoring period (Fig. 4a). We estimated the percentage of PF occurrence at a specific horizon as: (PF occurred in a horizon)/ (PF occurred in the entire soil profile) \times 100%. From such an estimation, we identified that PF occurred favorably in some specific horizons (rather than evenly distributed among various horizons in a soil profile) (Fig. 4b). For instance, 58.5 and 62.6% of the PF at Site U1 were observed at the interface of the AC-R horizons and in the R horizon, respectively, but <10.2% occurred in each of the other horizons in that soil profile (A and CR horizons). At Site M2b, >90% of the PF occurred in the A horizon, and <10% occurred in other horizons (Fig. 4b). When comparing the periods of 2007 to 2009 vs. 2010 to 2012, a matched-pair t-test suggested that there was no significant difference in their frequencies of PF occurrence (t = 0.91, p = 0.39), indicating statistical consistency in PF frequency during the entire 5.5-yr period. Such consistency was also observed in the indices that controlled PF occurrence (Table 2; Fig. 5). Relatively good agreement (>60%) was observed in those indices between the two monitoring periods (2007–2009 vs. 2010–2012), especially for the upslope sites (U1, U2a, and U2b) and the lower slope sites (L1a, L1b, and L2), where the agreement of the PFgenerating indices reached >80% (Fig. 5).

Despite the overall consistency, however, some slight differences were also observed. For example, precipitation kurtosis seemed significant for the 175 events during 2007 to 2009 (significant at \geq 5 sites) but was less so for the 323 events during 2007 to 2012 (Table 2). Only nine indices were identified as significant controls of widespread PF occurrence for the 175 events during 2007 to 2009 (e.g., time, amount and average intensity to maximum intensity, time to maximum event CPI9, day of year, and the profile average and depth-weighted average of initial soil moisture), whereas six additional indices (total precipitation, event duration, maximum event CPI99 or CPI999, and time to

maximum event CPI99 or CPI999) were also significant in controlling PF occurrence during 2007 to 2012 (Table 2). This is consistent with the conclusion made by Graham and Lin (2011), i.e., that while the frequency of PF occurrence may be determined from 1 yr of continuous monitoring, the controls on PF occurrence requires >3 yr of monitoring, thus confirming the value of long-term, in situ soil moisture monitoring.

Spatial Analysis at the Hillslope and Catchment Scales

No clear spatial pattern was observed in the frequency of PF occurrence at the hillslope scale (Fig. 3), but different controls on PF occurrence were observed at various topographic positions (Table 2). The upper slope sites (U1, U2a, and U2b) were insensitive to most of the precipitation indices but especially sensitive to the initial soil moisture condition (i.e., PF was more likely to occur in dry soils at these sites), air temperature (more PF occurrence with hot temperatures), and the day of the year (PF more likely to occur later in the year), all of which were related to hydrophobicity-induced PF. In comparison, the middle and lower slope sites were sensitive to both precipitation indices and initial soil moisture conditions (Table 2). We compared the PF occurrence frequency at the 10 sites along this hillslope during the period of May 2011 to June 2012 with the longer term results from the period of January 2007 to June 2012 and found no significant differences between the two periods (t = -0.21, p

= 0.98). Thus, 1 yr of monitoring appeared to be sufficient to determine the frequency of PF occurrence at this scale in this catchment, which is consistent with our previously published results (Graham and Lin, 2011).

By adding 25 more sites, we determined the frequency of PF occurrence across the entire catchment during the periods from May 2011 to June 2012 (with a total of 69 delineated precipitation events) and from July 2012 to July 2013 (with a total of 87 delineated events). The overall averaged frequency of PF occurrence was 25.7 and 26.0% for the 2011 to 2012 and 2012 to 2013 periods, respectively, with their ranges also similar (from <1 to 70.1% for 2011–2012 and from 2.9 to 72.4% for 2012–2013). Higher averaged frequency of PF occurrence was observed at the sites on the hilltop (45.8%), valley floor (47.6%), and swales near the stream (39.6%), while lower averaged frequency of PF was found at the sites on planar hillslopes (16.5%) and convex hillslopes (16.9%) (Fig. 1). Like that at the hillslope scale, widespread PF occurrence across the catchment was not common

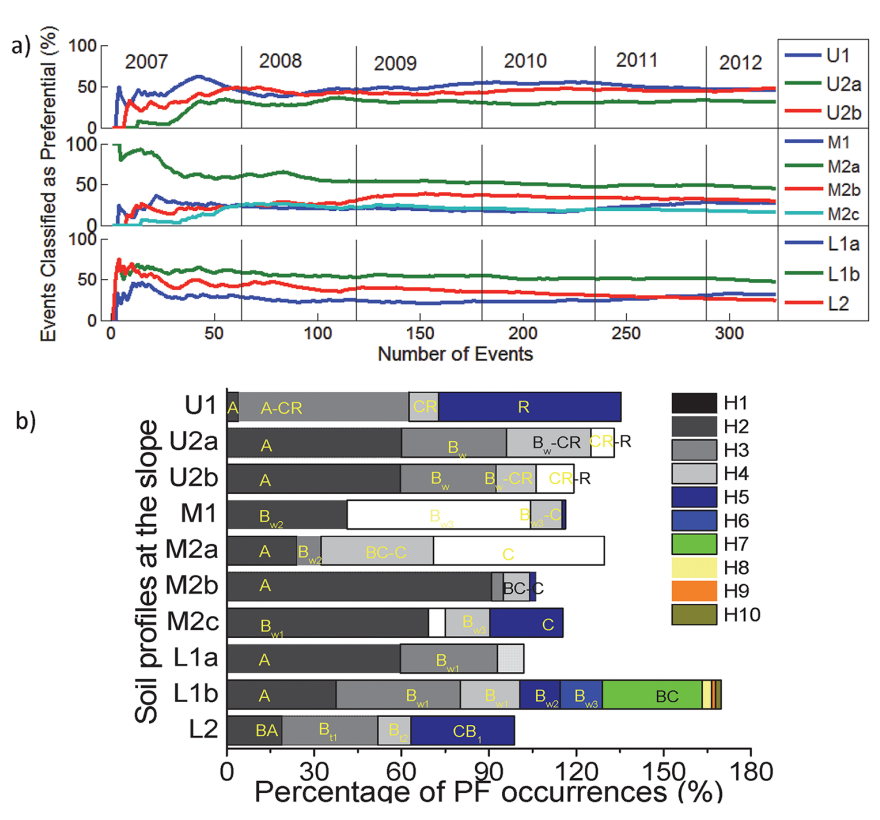


Fig. 4. (a) Percentage of precipitation events identified as causing preferential flow (PF) vs. the total number of events considered at each of the 10 monitoring sites installed before 2011. Vertical lines separate the events occurring in individual years from 2007 to 2012; (b) stacked bar chart of the percentage of PF occurrence at a specific soil horizon or horizon-horizon interface (with two horizons indicated) in each of the 10 monitoring sites along the hillslope. The total length of each bar stack indicates the cumulative percentage of PF occurrence throughout the entire soil profile with the 5.5-yr data. The different colors within each bar indicate the percentage of each horizon or horizon-horizon interface monitored (the percentage of PF occurrence in each horizon is <100% but the sum of multiple horizons could be >100%). In both figures, sites are organized from hilltop to hill bottom, with the ridgetop and hillslope sites (U1, U2a, and U2b) above the midslope sites (M1, M2a, M2b, and M2c) and above the lower swale and valley sites (L1a, L1b, and L2). The colored legend on the right in (b), H1 through H10, refers to different soil horizons from the top to the bottom in each profile. Soil horizons with relatively large PF frequency are marked with pedogenic symbols.

(e.g., only 7% of delineated events triggered PF at ≥ 20 sites, and no event generated PF at ≥ 30 sites) (Table 4). Interestingly, the overall frequency distribution of PF occurrence across the catchment revealed a possible hidden subsurface flow network in this catchment, as depicted in Fig. 1b, which was associated with two main swales in the catchment (one on the south-facing hillslope and the other on the north-facing hillslope).

Soil and Topographic Control on Preferential Flow Occurrence

At the hillslope scale, no obvious difference in the frequency of PF occurrence was detected among different topographic positions, nor was there strong evidence supporting the topographic control on PF occurrence frequency (Fig. 3). The Spearman correlations were poor between PF occurrence frequency and topography-related features at this hillslope scale, including slope ($r_{\rm s}=-0.21, p>0.05$), curvature ($r_{\rm s}=0.22, p>0.05$), soil depth ($r_{\rm s}=-0.26, p>0.05$), and upslope contributing area ($r_{\rm s}=0.27, p>0.05$).

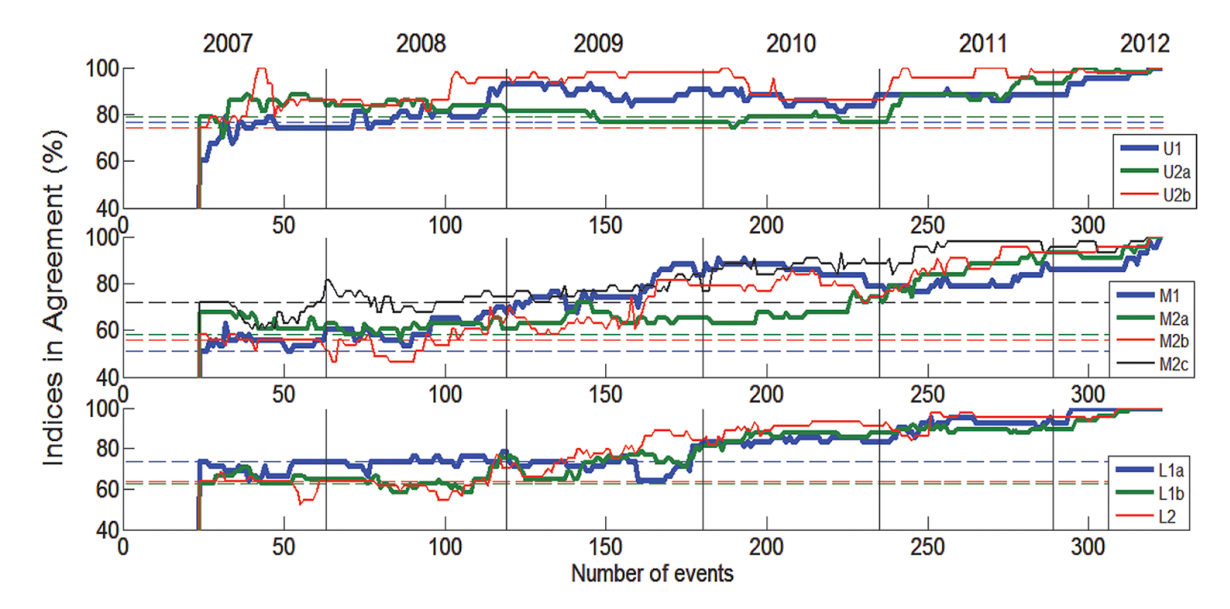


Fig. 5. Agreement on the controls of preferential flow (PF) occurrence as identified from 24 to 323 precipitation events from January 2007 to June 2012 at each of the 10 monitoring sites installed at the hillslope scale. Complete agreement on the identified controls of PF occurrence with those identified from all 323 events is indicated as 100% (i.e., <100% agreement means the controls identified from the subset data have not reached a perfect match with those identified from the entire data set of 323 events). Horizontal dashed lines of the same color show the agreement percentage (largely 50–80%) if no indices were determined as significant (i.e., null hypothesis, which depends on the number of significant indices identified for each site). Sites are organized from the hilltop to the hill bottom, with the ridgetop and hillslope sites (U1, U2a, and U2b) above the midslope sites (M1, M2a, M2b, and M2c), and above the lower swale and valley sites (L1a, L1b, and L2). Vertical lines separate the events occurring in individual years from 2007 to 2012.

At the catchment scale, however, we observed a clearer trend in the frequency of PF occurrence among different landform units and soil types (Fig. 6; Table 4). It is apparent that the south-facing sites overall had a higher frequency of PF occurrence than the north-facing sites, regardless of soil type and landform unit, but such differences generally were not statistically significant at the p < 0.05 level (Fig. 6). When comparing different soil series, a large range of PF occurrence frequency was observed in the Weikert and

Rushtown soil series (<1–70.1% for the Weikert and 1.7–53.7% for the Rushtown), which was associated with varying terrain attributes within these two soil series (Fig. 1; Table 1) as well as varying initial soil moisture conditions at different times of a year (Table 2). Overall, the Ernest soils on the valley floor and the Weikert soils on the ridgetop had higher frequencies of PF occurrence (Fig. 6a).

Across the catchment, relatively distinct patterns were detected among different landform units (Fig. 6b). The sites on

Table 4. Percentage of precipitation events leading to each of the three flow regimes (preferential flow, sequential flow, and non-detectable response) at different numbers of sites among the 35 sites of the entire catchment or the sites on south- or north-facing hillslopes or valley floor based on 69 precipitation events that occurred from May 2011 to June 2012.

					Percent	age of events resulting in each flow scenario									
Flow type	≥1 site	≥ 2 sites	≥ 3 sites	≥4 sites	≥5 sites	≥6 sites	≥7 sites	\geq 8 sites	≥9 sites	≥10 sites	≥15 sites	≥20 sites	≥30 sites	≥35 sites	
								% ———							
						<u>Enti</u>	re catchn	nent (35 s	ites)						
Preferential flow	94	77	68	65	61					42	14	7	0	0	
Sequential flow	97	84	75	74	70					52	35	9	0	0	
Nondetectable	71	55	54	51	51					46	39	33	12	0	
	South-facing hillslopes (17 sites)														
Preferential flow	93	75	61	54	41	33	20	10	6	3					
Sequential flow	93	75	71	59	54	51	41	26	19	10					
Nondetectable	59	52	52	51	45	41	35	35	33	30					
						North-	facing hil	Islopes (1	3 sites)						
Preferential flow	62	55	41	23	12	9	7	6	3	0					
Sequential flow	70	65	62	54	51	46	42	35	23	4					
Nondetectable	55	49	48	46	43	41	41	38	35	33					
	Valley floor (5 sites)														
Preferential flow	64	52	43	17	0										
Sequential flow	3	1	0	0	0										
Nondetectable	48	45	9	0	0										

the hilltop and on the valley floor had the highest frequency of PF occurrence, while the swale and convex hillslope sites had a slightly higher averaged frequency of PF occurrence than the planar hillslopes (Fig. 6b). However, the correlation analysis between PF occurrence frequency and the topographic indices showed no significant relationship with any individual terrain attribute (p > 0.05) except slope, which showed a moderately significant correlation with PF occurrence frequency ($r_{\rm s} = 0.42, p < 0.01$).

Spatial Variance and Dependence

A significantly larger range of PF occurrence frequency was observed at the catchment scale (<1–70%) than the hillslope scale (16–47%). Spatial variance was evident as the PF occurrence could vary significantly among even the closest sites (e.g., averaged PF frequency was 45, 29, and 16% at the three closely located Sites M2a, M2b, and M2c). However, evidence also suggested a clear spatial pattern of PF occurrence that may reflect a hidden subsurface flow network in this catchment (Fig. 1b). We used regression kriging to interpolate the observed frequency of PF occurrence to the entire catchment (Fig. 1b), where local slope (S, %), soil depth (D, in cm), profile-averaged sand content (SA, % w/w) and silt content (ST, % w/w) were selected by stepwise regression as the main attributes affecting PF frequency: PF frequency (%) = 74.84 – 0.68S – 0.32SA – 2.02ST + 0.75D, R^2 = 0.32, p < 0.05.

The interpolated map (with data collected at all the listed depths for the 35 sites; Table 1) showed a clear pattern of PF occurrence in the entire catchment (Fig. 1b). Hilltops and the valley floor had higher frequencies of PF occurrence, but these areas were relatively small compared with the entire catchment. Swales were the dominant areas of PF occurrence. Compared with the PF frequency determined from all the monitored depths in all the soil profiles, the PF frequency estimated with the data selected from only three main horizons (mostly A, B, and C horizons; see Table 1) were largely the same or slightly lower (with few substantially lower), depending on site-specific soil features. However, the overall spatial pattern of PF occurrence throughout the catchment and the hidden subsurface flow network revealed remained similar to that obtained from all the monitored depths.

To test whether the revealed spatial pattern of PF occurrence in the catchment was consistent, the most recent data set from July 2012 to July 2013 was used. The difference in PF occurrence frequency between 2011–2012 and 2012–2013 was statistically insignificant by paired t-test (p > 0.05), and the overall spatial patterns between the 2 yr looked quite similar. The overall average and the range between the 2 yr were also quite similar: 25.7% average with <1 to 70.1% range for 2011–2012 and 26.0% average with 2.9 to 72.4% range for 2012–2013.

Spatial Estimation of Preferential Flow Occurrence

Multiple linear regression equations obtained through the stepwise algorithm were tested for their estimation of PF occur-

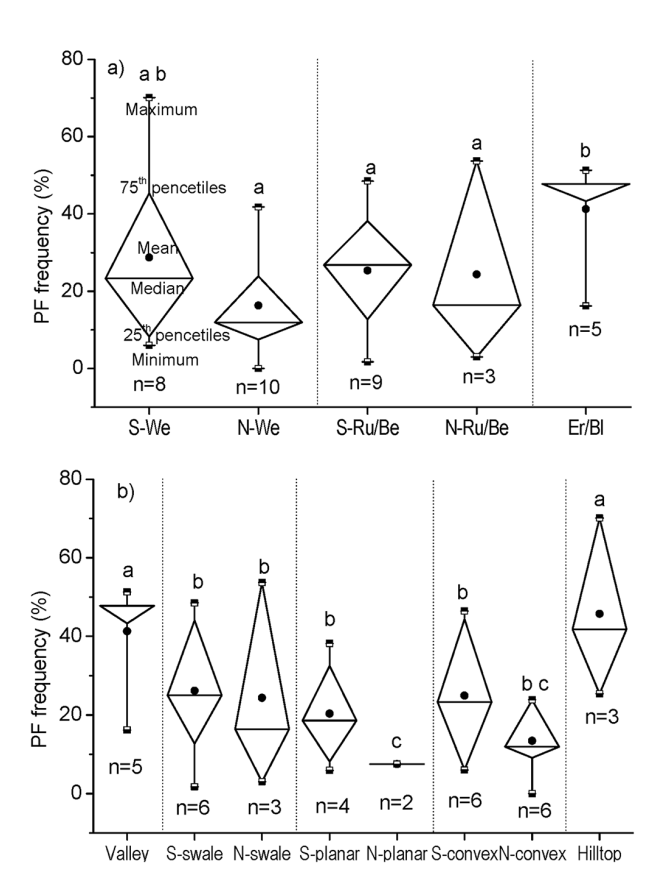


Fig. 6. Box-and-whisker diagrams showing the minimum, median, 25th percentile, 75th percentile, and the maximum frequency of preferential flow occurrence as determined from the 69 precipitation events that occurred from May 2011 to June 2012. These sites are based on all the soil moisture monitoring sites listed in Table 1, grouped by (a) soil series (We, Weikert; Ru/Be, Rushtown/Berks; Er/Bl, Ernest/Blairton) and hillslope aspects (S, south-facing hillslopes; N, north-facing hillslopes) and (b) landform units (valley, swale, planar hillslope, convex hillslope, and hillslop and hillslope aspects (S, south-facing; N, north-facing); n refers to the number of sites. Different letters indicate significant differences (p < 0.05) according to Duncan's multiple range tests.

rence using soil-terrain attributes. Two equations were identified (Table 5), one for the hillslope scale based on the data collected from 2007 to 2012 (10 sites) and the other for the catchment scale based on the data collected from 2011 to 2012 (35 sites). The estimations based on these two equations were compared modestly with the latest field data collected from July 2012 to July 2013 (Fig. 7), with R^2 of 0.4868 and 0.4325 for the hillslope and the catchment scales, respectively (both statistically significant). As the scale changed from the hillslope to the catchment, the overestimation using soil-terrain attributes at the hillslope scale crossed over the 1:1 line (i.e., changed from overestimation at low-frequency PF occurrence to underestimation at higher frequency PF occurrence; Fig. 7), whereas the main controlling variables changed from curvature and soil clay content to slope, soil depth, and soil sand and silt contents (Table 5). Apparently, there is a limit to this kind of estimation using static soil-terrain attributes because many more factors are involved in PF dynamics, such as temporal controls associated with precipitation characteristics and initial soil moisture. Such complexity is further discussed below.

DISCUSSION

Temporal Controls and Consistency in Preferential Flow Occurrence

Precipitation characteristics and initial soil moisture were the two main temporal controls on PF occurrence, as revealed in this study and in many other published works (e.g., Hutchinson and Moore, 2000; Kim et al., 2005; Tromp-van Meerveld and McDonnell, 2006; Lin and Zhou, 2008; Graham and Lin, 2011). The occurrence of subsurface PF, especially lateral subsurface flow, requires sufficient moisture inputs and the passing of a rainfall threshold to initiate in the valley floor and swales but is prominently promoted by dry conditions at the hilltop associated with soil hydrophobicity and/or cracking (Uchida et al., 2005; Lin and Zhou, 2008). While the controlling precipitation factors varied among the individual sites, the overall features of precipitation that favored widespread PF occurrence in the catchment seemed relatively stable, mainly total precipitation and its duration, the antecedent precipitation index for 1 d (API 1), time to maximum precipitation event (CPIs), and current precipitation index with a recession coefficient of 0.99 (CPI99) (Table 2).

Different mechanisms were involved in initiating PF in various hillslope positions. Under dry conditions, shrinkage cracks and/or hydrophobicity were largely responsible for the observed PF at the hilltop sites (Table 2), through which the dry organic-coated soil matrix could be more easily bypassed (Lin and Zhou, 2008; Cuthbert et al., 2010). Under wet conditions, the buildup of local saturation could connect macropores that resulted in an efficient network to deliver water downslope (Sidle et al., 2001; Negishi et al., 2007; Anderson et al., 2009; Beven and Germann, 2013). Consequently, PF occurred more often at the valley floor and swale sites under wet conditions (Lin, 2006; Lin and Zhou, 2008).

Air temperature was significant in controlling the occurrence of PF in most sites at the hillslope scale but was not significant for widespread PF initiation (Table 2). This phenomenon was due to the strong correlation between air temperature and initial soil moisture, and the contrasting mechanisms involved in PF occurrence at the upper vs. lower hillslope sites (Graham and Lin, 2011). Our data revealed an overall higher frequency of PF occurrence in most hillslope sites during the dry season and a strong relationship between PF occurrence frequency and the day of the year (Fig. 3; Table 2). This could be attributed to the coincidence of the high air temperature, low soil moisture, and more intense precipitation in late summer to early fall in our study area (Graham and Lin, 2011). There was a relative consistence in the frequency of PF occurrence at the hillslope scale throughout the 5.5 yr from 2007 to 2012, which was attributed to (i) considerable statistical stability of the precipitation distribution during the entire monitoring period (Fig. 2) and (ii) relatively stable PF flowpaths, as observed in our field studies and revealed by our monitoring data (e.g., Lin, 2006). For example, PF occurrence was dominant in some specific horizons or horizon interfaces rather than being evenly distributed throughout the soil profiles, as shown in Fig. 4b. Other studies have also shown that PF flowpaths reoccurred at the same locations during successive storm events and remained stable for a period of time without anthropogenic disturbance (de Rooij, 2000; Ritsema et al., 2000; Hagedorn and Bundt, 2002). The observed temporal consistency of PF is an important characteristic of hillslope hydrology and biogeochemistry, as this can help identify differences in biological and chemical conditions between PF flowpaths and the surrounding soil matrix (Bogner et al., 2012).

Spatial Controls and Dependence in Preferential Flow Occurrence

Significant differences were found in the occurrence frequency of PF among different landform units and soil types (Fig. 6). A higher frequency of PF occurrence was detected at the hilltop (average 45.6%) and the valley floor (40.7%), while the overall frequency for swales was 25.6% and that for planar and convex hillslopes was 18.1%. Higher PF frequency at the hilltop and the valley floor are explained by the topographically controlled soil moisture conditions. While there were some differences among the soil types in terms of their frequency of PF occurrence, especially for the Ernest and Blairton soil series located on the valley floor, the other three soil series located on the hillslopes and hilltops (i.e., the Weikert, Berks, and Rushtown series) were better differentiated using the type of hillslopes (i.e., concave, convex, or planar) and aspects (i.e., south- vs. north-facing) (Fig. 6a). It is evident that soil series alone is insufficient here to explain the variation observed in PF occurrence frequency.

As expected, when upscaling to the catchment scale, the topographic control on PF occurrence was amplified. An obvious spatial pattern was noticeable, especially when looking at the interpolated map of PF occurrence frequency that revealed a probable hidden subsurface PF network (Fig. 1b). A statistically significant, but only moderate, correlation was observed between PF frequency and local slope (p < 0.01, $r_{\rm s} = 0.42$). Except for this, we did not find a significant simple correlation between PF frequency and the other individual terrain attributes, including altitude, curvature, upslope contributing area, and topographic wetness index (p > 0.05). We also did not find a significant correlation between PF frequency and soil thickness or other individual soil properties (e.g., profile-averaged rock, sand, silt, and clay contents) (p > 0.05). However, combining multiple soil-terrain attributes (as done in the multiple regression shown

Table 5. Parameter coefficients for multiple linear regression equations obtained through stepwise regression for predicting preferential flow occurrence frequency at the hillslope scale (data from 2007–2012) and the catchment scale (data from 2011–2012). The relative importance of the selected variables were based on *t* values.

	Par				Relative importance of						
Scale	Intercept	Slope	Curvature	Soil depth	Sand	Silt	Clay	n	R^2	p	selected variables
Hillslope (Eq. [1])	28.12		32.65				1.64	10	0.81	< 0.01	curvature > clay
Catchment (Eq. [2])	74.84	-0.68		0.75	-0.32	-2.02		35	0.32	< 0.05	slope > sand > depth > silt

in Table 5), moderate estimation accuracy of PF occurrence was achieved (Fig. 7). It was the interplay between landform units and soil types, coupled with initial soil moisture and precipitation features, that determined the initiation and persistency of PF occurrence in this catchment.

Uncertainty Analysis

As summarized by Clothier et al. (2008), Lin (2010), and others, PF may occur at all spatial and temporal scales, but no simple deterministic scheme may fully capture the complexity involved. One uncertainty encountered in this study lies in the fact that each soil moisture probe can monitor only a small volume in heterogeneous soils where irregular flow patterns may occur. Should more sensors be installed in each soil profile, they may capture a higher likelihood of PF. In addition, PF may occur more frequently at some interfaces of soil layers, but not all of the interfaces were installed with soil moisture sensors in this study. This implies a possible underestimation of PF occurrence as reported here. On the other hand, possible disturbance caused by probe installation may introduce unnatural PF (this is a pure speculation based on the uncertainty principle). However, every effort was made in this study to avoid or minimize such a possibility (e.g., all the sensors were installed in the upslope direction above the soil pits; all cables were carefully buried below the depth of the installed probes and then laid horizontally away from the probe locations; and all the soil pits were carefully refilled with the original soils layer by layer). Nevertheless, given the large number of probes that we installed and the extensive spatial coverage (35 sites throughout the catchment), plus 6.5 yr of monitoring, we are confident about the general pattern of PF occurrence captured in this study. This is further supported by the overall similarity of the PF occurrence throughout the catchment between the years of 2011-2012 and 2012-2013.

Aside from the uncertainties associated with soil moisture measurements, uncertainties could also be introduced by precipitation measurements. In this study, we used the averaged value of throughfall from six rain gauges installed underneath the canopy to delineate precipitation events, but the volume of rainwater that actually reached the ground surface may be altered differently at different sites by canopy interception with different tree species and sizes, and thus may cause some degree of rainfall heterogeneity across the catchment (Brauman et al., 2010). The spatial distribution of throughfall could also change with the seasonal dynamics of the forest canopy. However, only a slight, insignificant difference was found among our various rain gauges (such slight difference was partially attributed to canopy influence and occasional clogging by fallen leaves). Vegetation (especially tree roots, stemflow, and litterfall) as a likely control on PF occurrence has not been examined in this study (e.g., stemflow may trigger PF, and the position of soil moisture monitoring sites relative to tree and root locations may also impact PF occurrence). We have now mapped out the distribution of tree species and their sizes throughout the entire catchment, which provides the necessary data sets to begin this investigation in the next step.

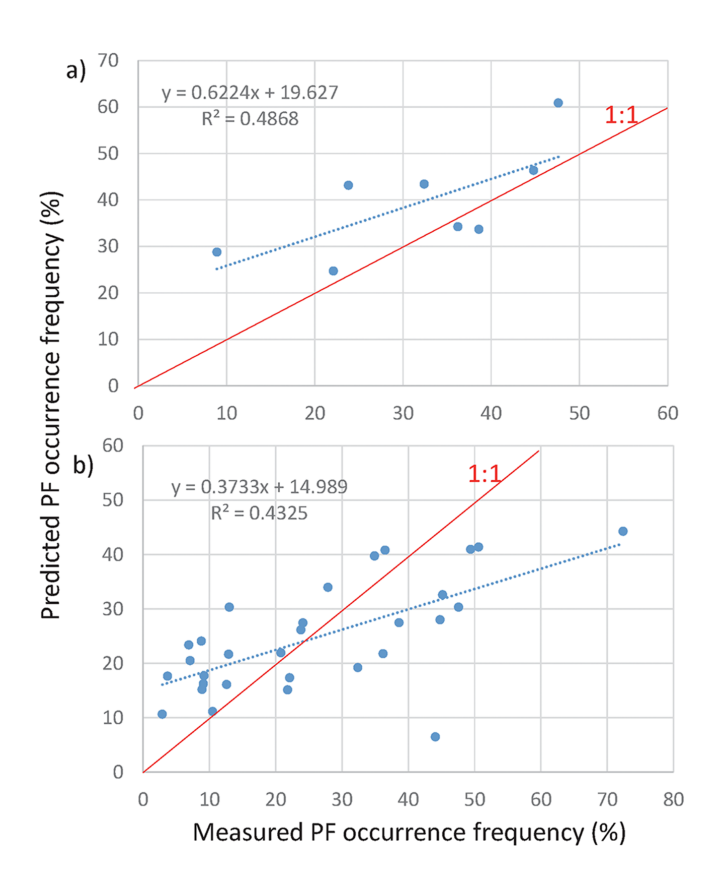


Fig. 7. Predicted preferential flow (PF) occurrence frequency based on the past several years' data vs. measured PF frequency from the latest year's data (2012–2013): (a) prediction based on the hillslope-scale data (10 sites) collected from 2007 to 2012 using the regression Eq. [1] in Table 5, and (b) prediction based on the catchment-scale data (35 sites) collected from 2011 to 2012 using the regression Eq. [2] in Table 5.

Some studies elsewhere have reported possible links between vegetation and PF occurrence (e.g., Sarkar et al., 2008; Li et al., 2009; Archer et al., 2012). The connection between the distribution pattern of vegetation and the organization of PF flowpaths could provide additional insights into the links between ecohydrology and hydropedology for subsurface flow (Li et al., 2009; Mueller et al., 2010).

Implications of the Results from This Study

The temporal consistency and spatial dependence of PF occurrence in the Shale Hills illustrate a probable hidden subsurface PF network that is spatially structured but temporally dynamic. It has been recognized that individual short PF pathways may be linked via a series of nodes in a network, which may be switched on or off and expand or shrink depending on local soil moisture conditions, rainfall inputs, and plant activities, thus forming dynamic PF networks (e.g., Sidle et al., 2001; Gish et al., 2005; Guo et al., 2014). With time, these networks may self-organize, thus forming temporally stable PF pathways (analogous to stream network organization). Our extensive ground penetrating radar scanning of the catchment and related infiltration experiments and water stable isotope data have provided supports for the observed subsurface PF network (e.g., Doolittle et al., 2012; Thomas et al., 2013; Zhang et al., 2014; Guo et al., 2014).

We note that, although PF pathways may be relatively stable, PF itself is highly dynamic depending on initial soil moisture, precipitation features, and vegetation dynamics. Our results suggest complex interactions among these factors, together with landform units and soil types. It has been debated that PF may be essentially unpredictable because the geometry and properties of conducting macropores and other PF flow paths are generally unknown and the dynamic connectivity of various PF pathways in the subsurface remains poorly understood (Beven, 1991; Jury and Flühler, 1992). Although a lot has happened since the 1980s and 1990s, with considerable work done related to PF (Beven, 2010; Beven and Germann, 2013), many variables that substantially affect PF occurrence remain poorly known in different landscapes (e.g., interfaces of various soil layers, the continuity and connectivity of flow paths, and temporal changes in flow itself vs. flow paths). Nevertheless, Jarvis et al. (2009) suggested that knowing the integrated effect of PF is more important than precisely knowing the behavior of individual PF pathways. Through a simple classification scheme for predicting the susceptibility of soil horizons and pedons to PF, Jarvis et al. (2009) concluded that PF paths were actually predictable to a sufficient degree. Our results reported here suggest that there is a moderate but limited degree of possibility in estimating PF occurrence using static soil-terrain attributes. We believe that developing an appropriate classification scheme of various major controls on PF occurrence in diverse soil landscapes would be a meaningful pathway forward to enhance PF prediction and modeling.

How might the results from this study be useful to enhance PF modeling? Several aspects may be considered in this regard:

- The statistics of PF occurrence frequency in different landforms and soils, as reported in this study, can provide a relatively explicit account of where and when PF might be significant in a given landscape.
- The use of some classification schemes of the main controls on PF occurrence, such as initial soil moisture and precipitation features, can provide a guide to estimating the likelihood of PF occurrence under different climatic conditions.
- The soil-terrain-based deterministic component of PF occurrence must be combined with the precipitation- and initial-moisture-based stochastic component in modeling PF dynamics.
- The hidden subsurface PF network inferred in this study suggests that a network-based approach may be useful in modeling PF (Lin, 2010; Graham and Lin, 2012).
- Enhanced geophysical tools (such as time-lapsed ground penetrating radar) may be used in combination with soil moisture monitoring to reveal dynamic PF networks, as demonstrated by Doolittle et al. (2012), Zhang et al. (2014), and Guo et al. (2014).

While there have long been physically based numerical attempts to model PF flows through soils, many challenges remain. Perhaps one of the most fundamental among these challenges is the dynamic partitioning and the interaction of flow domains between the more traditional porous portion of the soil and the PF domain. Thus, developing an integrated modeling system that can couple continuum-based and network-based approaches may be an alternative way forward. This is because subsurface flow can often be described as complex PF networks embedded in soil-landscape mosaics (Lin, 2012; Graham and Lin, 2012).

The findings from this study also have implications for enhanced monitoring and modeling of "hot spots" (active locations) and "hot moments" (critical timing) in biogeochemical dynamics and nutrient cycling. Because hydrology often triggers "hot spots" and "hot moments" of biogeochemical reactions and ecological functions (e.g., Bundt et al., 2001; McClain et al., 2003), improved understanding and modeling of PF will have implications for enhanced determination of chemical fluxes and elemental budgets in soils and ecosystems. Interpretation of point measurements without knowing PF paths is now often questioned (e.g., Gottlein and Manderscheid, 1998; Netto et al., 1999) because the uncertainty of whether the soil solution is extracted from stagnant or high-velocity flowpaths makes it practically impossible to reliably determine mass flux rates. Additional complications arise in structured soils for reactive components due to locally variable chemical conditions. Furthermore, macropore linings and aggregate coatings could restrict lateral mass transfer and reduce sorption and retardation, hence physical and biochemical non-equilibriums are enhanced. All these suggest that there is a need to identify and model PF networks if we are to identify "hot spots" and "hot moments" of biogeochemistry in different landscapes.

SUMMARY AND CONCLUSIONS

Through quantifying the frequency and controls of PF occurrence in the Shale Hills Catchment from pedon to catchment scales, this study has provided further insights regarding where and when PF may be important. Our extensive soil moisture monitoring revealed a probable hidden subsurface flow network across the 7.8-ha forested catchment, which is linked to soil-landscape features (especially swales). Selected soil-terrain attributes provided a moderate but limited capability for estimating PF occurrence at both the hillslope and catchment scales.

Of the total 323 precipitation events that occurred from 2007 to 2012, 16 to 47% generated PF at each of the 10 sites at the hill-slope scale, whereas the 69 precipitation events from May 2011 to June 2012 and the 87 events from July 2012 to July 2013 generated an overall-averaged 26% PF occurrence frequency across the entire catchment (with a range from <1 to $\sim\!\!70\%$). Considerable temporal consistence was found in both the occurrence and the main controls of PF at the hillslope scale; however, no significant difference in PF occurrence frequency was detected among the sites at different hillslope positions. Intense precipitation overall facilitated PF generation, while the specific characteristics of precipitation events that induced PF seemed to be site specific. Preferential flow occurrence was clearly sensitive to initial soil moisture, favoring dry soils at upslope sites and wet soils in downslope areas.

When upscaling to the catchment scale, topographic controls on PF occurrence as well as their spatial pattern became more evident. The overall spatial pattern revealed a subsurface flow network in the catchment that remained fairly similar between the two full years for which we have collected data (i.e., 2011-2012 and 2012–2013). The spatial pattern showed that the south-facing hillslopes had a higher overall frequency of PF occurrence than the north-facing hillslopes, and the hilltops and the valley floor had a greater chance of PF occurrence than the middle of the hillslopes. However, except slope, no simple correlation was found between PF occurrence frequency and other individual soil or terrain attributes. Nevertheless, the swales overall had a higher frequency of PF occurrence, while the convex and planar hillslopes had the least chance of experiencing PF. Such a spatial pattern was consistent with a temporally stable and spatially organized subsurface PF network in this catchment. The hidden subsurface PF network revealed in this study is apparently controlled jointly by the complex interactions among landform units, soil types, initial soil moisture conditions, precipitation features, and seasons.

Overall, the observed temporal consistency and spatial dependence of PF occurrence in this humid temperate catchment can enhance our understanding and estimation of subsurface PF occurrence in complex terrains and shed light on the statistical frequency and dominant controls of PF occurrence in this and other similar forested landscapes. We suggest continued efforts in quantifying PF occurrence and controls in different landscapes using soil moisture sensor networks, which have become increasingly available worldwide, and could lead to a more comprehensive understanding of PF and its modeling and prediction across diverse landscapes.

ACKNOWLEDGMENTS

This research was supported in part by the National Science Foundation Hydrologic Sciences Program (Grant EAR-1416881) and the Critical Zone Observatory Program (EAR-0725019, PI: C. Duffy; and EAR 1239285, EAR 1331726, PI: S. Brantley). This work was conducted in Penn State's Stone Valley Forest, which is supported and managed by the Penn State's Forestland Management Office in the College of Agricultural Sciences. Assistance in the field data collections and maintenance from the Penn State Hydropedology Group is gratefully acknowledged, especially Bob Zhou, Chris Graham, Jun Zhang, and Isaac Hopkins.

REFERENCES

- Alaoui, A., U. Caduff, H.H. Gerke, and R. Weingartner. 2011. Preferential flow effects on infiltration and runoff in grassland and forest soils. Vadose Zone J. 10:367–377. doi:10.2136/vzj2010.0076
- Allaire, S.E., S. Roulier, and A.J. Cessna. 2009. Quantifying preferential flow in soils: A review of different techniques. J. Hydrol. 378:179–204. doi:10.1016/j.jhydrol.2009.08.013
- Anderson, A.E., M. Weiler, Y. Alila, and R.O. Hudson. 2009. Dye staining and excavation of a lateral preferential flow network. Hydrol. Earth Syst. Sci. 13:935–944. doi:10.5194/hess-13-935-2009
- Archer, N.A.L., J.N. Quinton, and T.M. Hess. 2012. Patch vegetation and water redistribution above and below ground in south-east Spain. Ecohydrology 5:108–120. doi:10.1002/eco.210
- Beven, K. 1991. Modeling preferential flow: An uncertain future? In: T.J. Gish and A. Shirmohammadi, editors, Preferential flow. Am. Soc. Agric. Eng., St. Joseph, MI. p. 1–11.
- Beven, K.J. 2010. Preferential flows and travel time distributions: Defining

- adequate hypothesis tests for hydrological process models. Hydrol. Processes 24:1537–1547. doi:10.1002/hyp.7718
- Beven, K., and P. Germann. 2013. Macropores and water flow in soils revisited. Water Resour. Res. 49:3071–3092. doi:10.1002/wrcr.20156
- Blume, T., E. Zehe, and A. Bronstert. 2009. Use of soil moisture dynamics and patterns at different spatio-temporal scales for the investigation of subsurface flow processes. Hydrol. Earth Syst. Sci. 13:1215–1233. doi:10.5194/hess-13-1215-2009
- Bogner, C., W. Borken, and B. Huwe. 2012. Impact of preferential flow on soil chemistry of a podzol. Geoderma 175–176:37–46. doi:10.1016/j.geoderma.2012.01.019
- Brauman, K.A., D.L. Freyberg, and G.C. Daily. 2010. Forest structure influences on rainfall partitioning and cloud interception: A comparison of native forest sites in Kona, Hawai'i. Agric. For. Meteorol. 150:265–275. doi:10.1016/j.agrformet.2009.11.011
- Bundt, M., F. Widmer, M. Pesaro, J. Zeyer, and P. Blaser. 2001. Preferential flow paths: Biological "hot spots" in soils. Soil Biol. Biochem. 33:729–738.
- Chappell, N.A. 2010. Soil pipe distribution and hydrological functioning within the humid tropics: A synthesis. Hydrol. Processes 24:1567–1581. doi:10.1002/hyp.7579
- Clothier, B.E., S.R. Green, and M. Deurer. 2008. Preferential flow and transport in soil: Progress and prognosis. Eur. J. Soil Sci. 59:2–13. doi:10.1111/j.1365-2389.2007.00991.x
- Cuthbert, M.O., R. Mackay, J.H. Tellam, and K.E. Thatcher. 2010. Combining unsaturated and saturated hydraulic observations to understand and estimate groundwater recharge through glacial till. J. Hydrol. 391:263–276. doi:10.1016/j.jhydrol.2010.07.025
- de Rooij, G.H. 2000. Modeling fingered flow of water in soils owing to wetting front instability: A review. J. Hydrol. 231–232:277–294. doi:10.1016/S0022-1694(00)00201-8
- Doerr, S.H., C.J. Ritsema, L.W. Dekker, D.F. Scott, and D. Carter. 2007. Water repellence of soils: New insights and emerging research needs. Hydrol. Processes 21:2223–2228. doi:10.1002/hyp.6762
- Doolittle, J., Q. Zhu, J. Zhang, L. Guo, and H. Lin. 2012. Geophysical investigations of soil-landscape architecture and its impacts on subsurface flow. In: H. Lin, editor, Hydropedology: Synergistic integration of soil science and hydrology. Academic Press, Waltham, MA. p. 413–447.
- Garré, S., J. Koestel, T. Günther, M. Javaux, J. Vanderborght, and H. Vereecken. 2010. Comparison of heterogeneous transport processes observed with electrical resistivity tomography in two soils. Vadose Zone J. 9:336–349. doi:10.2136/vzj2009.0086
- Gish, T.J., C.L. Walthall, C.S.T. Daughtry, and K.-J.S. Kung. 2005. Using soil moisture and spatial yield patterns to identify subsurface flow pathways. J. Environ. Qual. 34:274–286. doi:10.2134/jeq2005.0274
- Gottlein, A., and B. Manderscheid. 1998. Spatial heterogeneity and temporal dynamics of soil water tension in a mature Norway spruce stand. Hydrol. Processes 12:417–428.
- Graham, C., and H. Lin. 2011. Controls and frequency of preferential flow occurrence: A 175-event analysis. Vadose Zone J. 10:816–831. doi:10.2136/vzj2010.0119
- Graham, C.B., and H. Lin. 2012. Subsurface flow networks at the hillslope scale: Detection and modeling. In: H. Lin, editor, Hydropedology: Synergistic integration of soil science and hydrology., Academic Press, Waltham, MA. p. 559–593.
- Guo, L., H.S. Lin, and J. Chen. 2014. Subsurface lateral flow network on a hillslope revealed by time-lapse ground penetrating radar. Water Resour. Res. 50:9127–9147. doi:10.1002/2013WR014603
- Hagedorn, F., and M. Bundt. 2002. The age of preferential flow paths. Geoderma 108:119–132. doi:10.1016/S0016-7061(02)00129-5
- Hendrickx, J. M. H., and M. Flury. 2001. Uniform and preferential flow mechanisms in the vadose zone In: Conceptual models of flow and transport in the fractured vadose zone. Natl. Acad. Press, Washington, DC. p. 149–187.
- Hengl, T., G.B.M. Heuvelink, and D.G. Rossiter. 2007. About regression-kriging: From equations to case studies. Comput. Geosci. 33:1301–1315. doi:10.1016/j.cageo.2007.05.001
- Hutchinson, D.G., and R.D. Moore. 2000. Throughflow variability on a forested hillslope underlain by compacted glacial till. Hydrol. Processes 14:1751–1766. doi:10.1002/1099-1085(200007)14:10<1751::AID-HYP68>3.0.CO;2-U

- Jarvis, N.J. 2007. A review of non-equilibrium water flow and solute transport in soil macropores: Principles, controlling factors and consequences for water quality. Eur. J. Soil Sci. 58:523–546. doi:10.1111/j.1365-2389.2007.00915.x
- Jarvis, N.J., J. Moeys, J.M. Hollis, S. Reichenberger, A.M.L. Lindahl, and I.G. Dubus. 2009. A conceptual model of soil susceptibility to macropore flow. Vadose Zone J. 8:902–910. doi:10.2136/vzj2008.0137
- Jaynes, D.B., S.I. Ahmed, K.-J.S. Kung, and R.S. Kanwar. 2001. Temporal dynamics of preferential flow to a subsurface drain. Soil Sci. Soc. Am. J. 65:1368–1376. doi:10.2136/sssaj2001.6551368x
- Jury, W.A., and H. Flühler. 1992. Transport of chemicals through soil: Mechanisms, models, and field applications. Adv. Agron. 47:141–201. doi:10.1016/S0065-2113(08)60490-3
- Kemper, W.D., and E.J. Koch. 1966. Aggregate stability of soils from western United States and Canada: Measurement procedure and correlations with soil constituents. Tech. Bull. 1355. U.S. Gov. Print. Office, Washington, DC.
- Kienzler, P.M., and F. Naef. 2008. Subsurface storm flow formation at different hillslopes and implications for the 'old water paradox'. Hydrol. Processes 22:104–116. doi:10.1002/hyp.6687
- Kim, H.J., R.C. Sidle, and R.D. Moore. 2005. Shallow lateral flow from a forested hillslope: Influence of antecedent wetness. Catena 60:293–306. doi:10.1016/j.catena.2004.12.005
- Kulasekera, P.B., and G.W. Parkin. 2011. Influence of the shape of inter-horizon boundary and size of soil tongues on preferential flow under shallow groundwater conditions: A simulation study. Can. J. Soil Sci. 91:211–221. doi:10.4141/cjss10079
- Lago, M.E., F. Miralles-Wilhelm, M. Mahmoudi, and V. Engel. 2010. Numerical modeling of the effects of water flow, sediment transport and vegetation growth on the spatiotemporal patterning of the ridge and slough landscape of the Everglades wetland. Adv. Water Resour. 33:1268–1278. doi:10.1016/j.advwatres.2010.07.009
- Li, X., Z. Yang, Y. Li, and H. Lin. 2009. Connecting ecohydrology and hydropedology in desert shrubs: Stemflow as a source of preferential flow in soils. Hydrol. Earth Syst. Sci. 6:1551–1580. doi:10.5194/hessd-6-1551-2009
- Lin, H. 2006. Temporal stability of soil moisture spatial pattern and subsurface preferential flow pathways in the Shale Hills Catchment. Vadose Zone J. 5:317–340. doi:10.2136/vzj2005.0058
- Lin, H.S. 2010. Linking principles of soil formation and flow regimes. J. Hydrol. 393:3–19. doi:10.1016/j.jhydrol.2010.02.013
- Lin, H.S., editor. 2012. Hydropedology: Synergistic integration of soil science and hydrology. Academic Press, Waltham, MA.
- Lin, H., and X. Zhou. 2008. Evidence of subsurface preferential flow using soil hydrologic monitoring in the Shale Hills Catchment. Eur. J. Soil Sci. 59:34–49. doi:10.1111/j.1365-2389.2007.00988.x
- McClain, M.E., E.W. Boyer, C.L. Dent, S.E. Gergel, N.B. Grimm, P.M. Groffman, et al. 2003. Biogeochemical hot spots and hot moments at the interface of terrestrial and aquatic ecosystems. Ecosystems 6:301–312. doi:10.1007/s10021-003-0161-9
- Mueller, E.N., P. Hunke, P. Biro, and S. Jacobi. 2010. ECHO: Monitoring and analysis of ecohydrological feedback dynamics in three ecosystems. Annu. Rep. 2010. Inst. of Earth and Environ. Sci., Univ. of Potsdam, Potsdam, Germany.
- Negishi, J.N., S. Noguchi, R.C. Sidle, A.D. Ziegler, and A.R. Nik. 2007. Stormflow generation involving pipe flow in a zero-order basin of peninsular Malaysia. Hydrol. Processes 21:789–806. doi:10.1002/hyp.6271
- Netto, A.M., R.A. Pieritz, and J.P. Gaudet. 1999. Field study on the local variability of soil water content and solute concentration. J. Hydrol. 215:23–37.
- Oberdörster, C., J. Vanderborght, A. Kemna, and H. Vereecken. 2010. Investigating preferential flow processes in a forest soil using time domain reflectometry and electrical resistivity tomography. Vadose Zone J. 9:350– 361. doi:10.2136/vzj2009.0073
- Posadas, A., R. Quiroz, A. Tanus, S. Crestana, and C.M. Vaz. 2009. Characterizing water fingering phenomena in soils using magnetic resonance imaging and multifractal theory. Nonlinear Processes Geophys. 16:159–168. doi:10.5194/npg-16-159-2009
- R Development Core Team. 2005. R: A language and environment for statistical

- computing. R Foundation for Statistical Computing, Vienna.
- Ritsema, C. J., J. C. van Dam, J. L. Nieber, L. W. Dekker, K. Oostindie, T. S. Steenhuis. 2000. Preferential flow in water repellant sandy soils: Principles and modeling approaches. In: D. Bosch and K. King, editors, Preferential flow: Water movement and chemical transport in the environment, Proceedings of the 2nd International Symposium, Honolulu, HI. 3–5 Jan. 2001. Am. Soc. Agric. Eng., St. Joseph, MI. p. 129–132.
- Sammartino, S., E. Michel, and Y. Capowiez. 2012. A novel method to visualize and characterize preferential flow in undisturbed soil cores by using multislice helical CT. Vadose Zone J. 11(1). doi:10.2136/vzj2011.0100
- Sarkar, R., S. Dutta, and S. Panigrahy. 2008. Effect of scale on infiltration in a macropore-dominated hillslope. Curr. Sci. 94:490–494.
- Scherrer, S., F. Naef, A.O. Faeh, and I. Cordery. 2007. Formation of runoff at the hillslope scale during intense precipitation. Hydrol. Earth Syst. Sci. 11:907–922. doi:10.5194/hess-11-907-2007
- Sidle, R.C., S. Noguchi, Y. Tsuboyama, and K. Laursen. 2001. A conceptual model of preferential flow systems in forested hillslopes: Evidence of selforganization. Hydrol. Processes 15:1675–1692. doi:10.1002/hyp.233
- Šimůnek, J., N.J. Jarvis, M.Th. van Genuchten, and A. Gärdenäs. 2003. Review and comparison of models for describing non-equilibrium and preferential flow and transport in the vadose zone. J. Hydrol. 272:14–35. doi:10.1016/S0022-1694(02)00252-4
- Šimůnek, J., and M.Th. van Genuchten. 2007. Contaminant transport in the unsaturated zone: Theory and modeling. In: J.W. Delleur, editor, Handbook of groundwater engineering. 2nd ed. CRC Press, Boca Raton, FL.
- Takagi, K., and H.S. Lin. 2011. Temporal dynamics of soil moisture spatial variability in the Shale Hills Critical Zone Observatory. Vadose Zone J. 10:832–842. doi:10.2136/vzj2010.0134
- Takagi, K., and H.S. Lin. 2012. Changing controls of soil moisture spatial organization in the Shale Hills Catchment. Geoderma 173–174:289–302. doi:10.1016/j.geoderma.2011.11.003
- Thomas, E.M., H. Lin, C.J. Duffy, P.L. Sullivan, G.H. Holmes, S.L. Brantley, and L. Jin. 2013. Spatiotemporal patterns of stable isotope compositions at the Shale Hills Critical Zone Observatory: Linkages to subsurface hydrologic processes. Vadose Zone J. 12(4). doi:10.2136/vzj2013.01.0029
- Tromp-van Meerveld, H.J., and J.J. McDonnell. 2006. Threshold relations in subsurface stormflow: 2. The fill and spill hypothesis. Water Resour. Res. 42:W02411. doi:10.1029/2004WR003800
- Uchida, T., K. Kosugi, and T. Mizuyama. 2001. Effects of pipeflow on hydrological process and its relation to landslide: A review of pipeflow studies in forested headwater catchments. Hydrol. Processes 15:2151– 2174. doi:10.1002/hyp.281
- Uchida, T., I. Tromp-van Meerveld, and J.J. McDonnell. 2005. The role of lateral pipe flow in hillslope runoff response: An intercomparison of non-linear hillslope response. J. Hydrol. 311:117–133. doi:10.1016/j.jhydrol.2005.01.012
- Uhlenbrook, S., and J. Wenninger. 2006. Identification of flow pathways along hillslopes using electrical resistivity tomography (ERT). IAHS-AISH Publ. 303:15–20.
- Venables, W.N., and B. Ripley. 2002. Modern applied statistics with S. Springer, New York.
- Weiler, M., and H. Flühler. 2004. Inferring flow types from dye patterns in macroporous soils. Geoderma 120:137–153. doi:10.1016/j. geoderma.2003.08.014
- Zehe, E., and M. Sivapalan. 2009. Threshold behaviour in hydrological systems as (human) geo-ecosystems: Manifestations, controls, implications. Hydrol. Earth Syst. Sci. 13:1273–1297. doi:10.5194/hess-13-1273-2009
- Zhang, J., H.S. Lin, and J. Doolittle. 2014. Soil layering and preferential flow impacts on seasonal changes of GPR signals in two contrasting soils. Geoderma 213:560–569. doi:10.1016/j.geoderma.2013.08.035
- Zhao, Y., J. Tang, C. Graham, Q. Zhu, K. Takagi, and H. Lin. 2012. Hydropedology in the ridge and valley: Soil moisture patterns and preferential flow dynamics in two contrasting landscapes. In: H. Lin, editor, Hydropedology: Synergistic integration of soil science and hydrology. Academic Press, Waltham, MA. p. 381–411.
- Zhu, Q., and H.S. Lin. 2010. Interpolation of soil properties based on combined information of spatial structure, sample size and auxiliary variables. Pedosphere 20:594–606. doi:10.1016/S1002-0160(10)60049-5